

Article

Experimental Research for the Establishment of the Optimal Forging and Heat Treatment Technical Parameters for Special Purpose Forged Semi-Finishes

Nicolae Constantin ¹, Adrian Ioana ^{2,*} , Valentina Caloian ^{1,*}, Valeriu Rucai ¹, Cristian Dobrescu ¹, Alexandra Istrate ¹ and Vili Pasare ²

¹ Materials Science and Engineering Faculty, University Politehnica of Bucharest, 060042 Bucharest, Romania

² Engineering and Management of Metallic Materials Obtaining Department, Science and Engineering Materials Faculty, University Politehnica of Bucharest, 060042 Bucharest, Romania

* Correspondence: adyioana@gmail.com (A.I.); caloian_valentina@yahoo.com (V.C.)

Abstract: The authors present in this paper the experimental results and conclusions obtained after conducting a comparative study on three samples of forged semi-finished products from the steel brands 10CrMo9-10, 25CrMo4, and 42CrMo4. These are common heat-resistant alloy steels used in various industries nationally and internationally. This study aimed to test under the same identical experimental conditions of forging and heat treatment of three samples made of three different brands of steels 10CrMo9-10, 25CrMo4, and 42CrMo4. Analyzing the experimental results obtained, it can be seen for which of the three brands of tested steels the best forging and heat treatment parameters are obtained. Following experimental research, the best material was determined by analyzing the results obtained for the mechanical characteristics (tensile tests according to DNVGL-RP0034-SFC2 and NACE MR0175–hardness 207-235 HBW) and austenitic grain size. The authors determined that among the three types of steels analyzed, 10CrMo9-10 best meets the imposed requirements. This statement is in view of the comparative analysis of the results of experimental research.

Keywords: forging; heat treatment; steel; tempering; resilience; plasticity



Citation: Constantin, N.; Ioana, A.; Caloian, V.; Rucai, V.; Dobrescu, C.; Istrate, A.; Pasare, V. Experimental Research for the Establishment of the Optimal Forging and Heat Treatment Technical Parameters for Special Purpose Forged Semi-Finishes. *Materials* **2023**, *16*, 2432. <https://doi.org/10.3390/ma16062432>

Academic Editor: Andrea Di Schino

Received: 16 February 2023

Revised: 14 March 2023

Accepted: 15 March 2023

Published: 18 March 2023



Copyright: © 2023 by the authors. Licensee MDPI, Basel, Switzerland. This article is an open access article distributed under the terms and conditions of the Creative Commons Attribution (CC BY) license (<https://creativecommons.org/licenses/by/4.0/>).

1. Introduction

Production capacity utilization shall be calculated monthly based on gross steel production and information on the available capacity existing in the World Steel Association database [1–4].

The information submitted by the World Steel Association is based on publicly available data, updated twice a year, and verified by members of the World Steel Association [5,6]. The presence above certain limits of non-metallic inclusions in solidified steel ingots causes essential changes in their plasticity and hot deformation capacity due to the formation of structural discontinuities [7,8]. The mechanical properties of structural constituents are different and, therefore, during plastic deformation processes, do not deform evenly [9–11]. The interaction between the various deformed constituents leads to the appearance of tensions that can eventually lead to cracks or ruptures. The greater the difference between the mechanical properties of the various constituents, the greater the tendency to form discontinuities in the metal matrix [9].

The presence beyond certain limits of non-metallic inclusions in solidified steel ingots causes essential changes in their plasticity and thermic deformation capacity due to the formation of structural discontinuities [7–11]. Powdery and small ferrous waste resulting in different phases of industrial processes (in most cases steel) represents an intrinsic value, which is determined by the ferrous content (chemically bound iron, sometimes metallic) that can properly replace the raw material, namely iron ore/cast iron/scrap iron, in steel processes [6–8].

Since studying the absolute plastic properties of non-metallic inclusions is difficult to carry out, most experimental research sought to study the ability to deform non-metallic inclusions in the metal matrix, using relative indices comparing the plastic properties of non-metallic inclusions with those of steel in which they are included. To fully justify the need for experimental research, it should be mentioned that steel is currently one of the most used alloys in modern society [1,12–14].

Its versatility, durability, and resistance make it a popular choice for various fields: railway, machine building, naval, extractive, and chemical industries [15–19].

The forging of materials involves obtaining forged semi-finished in several successive stages and with a certain accepted deformation.

After applying the secondary heat treatment, an improved structure appears, which is no longer prone to cracks or the appearance of intergranular inclusions but is more fragile than the one obtained without secondary heat treatment [20–24].

The modeling of mechanical characteristics depends on the type of technological flow operations: free forging, primary TT, and secondary TT, but also on the chemical composition and the alloying elements of the steels used [25–28]. The novelty of the work is the performance of experimental research on samples of three different brands of steel, 10CrMo9-10, 25CrMo4, and 42CrMo4, subjected to forging and heat treatments under the same experimental conditions.

The research aims to find the best relationship between the resulting mechanical characteristics, heat treatment parameters, and the requirements of standards and international certification bodies.

Another novelty element is the exact establishment of a technology for the execution of a semi-finished product from 10CrMo9-10 with the best ratio of mechanical characteristics capable of meeting the conditions of international certification DNVGL-RP-0034-SFC2 and NACE MR0175 (maximum 22–23 HRC).

2. Materials and Method

2.1. Materials

To establish the best forging and heat treatment parameters of some forged semi-finished products, the authors performed comparative experimental research on 3 samples of forged semi-finished products from the steel brands 10CrMo9-10, 25CrMo4, and 42CrMo4.

The 10CrMo9-10 alloy steel specified in EN 10028-2 has good anti-corrosion properties and provides excellent performance with a higher Cr and Mo content that provides higher heat and corrosion resistance than 13CrMo4-5 and 16Mo3.

10CrMo9-10 is a high-temperature steel for pressure vessels and the transportation of petroleum products [29–32]. The chemical composition of the 10CrMo9-10 steel used in our own research is presented in Table 1.

Table 1. Chemical composition of 10CrMo9-10 [9].

C %	Mn%	Si%	P%	S%	Cr%	Mo%	Cu%
0.08	0.40	<0.50	<0.020	<0.010	2.00	0.90	<0.30
0.14	0.80				2.50	1.10	

25CrMo4 is a low-alloy steel that contains chromium and molybdenum as the main alloying elements. It is a versatile alloy with good resistance to atmospheric corrosion, strength, weldability, and processing characteristics. This steel is mainly used in the energy industry because it can be subjected to high temperatures, it has creep resistance.

Made parts: flanges, caps, nuts, turbines, toothed shafts. The chemical composition of the 25CrMo4 steel used in our own research is presented in Table 2.

Table 2. Chemical composition of 25CrMo4 [9].

C%	Si % max	Mn%	P% max	S%	Cr%	Mo%
0.22	0.40	0.60	0.025	0.035	0.90	0.15
0.29		0.90			1.20	0.20

The 42CrMo4 class steels are successful in the car construction industry, being used in the manufacture of high-resistance parts such as compressors, turbines, and working elements of heavy surface equipment. Steel has reduced weldability due to the high sensitivity to cracking. The chemical composition of the 42CrMo4 steel used in our own research is presented in Table 3.

Table 3. Chemical composition of 42CrMo4 [9].

C%	Si%	Mn%	P%	S%	Cr%	Mo%	Cu%
0.38	0.10	0.60	<0.025	<0.035	0.90	0.15	<0.40
0.45	0.40	0.90			1.20	0.30	

2.2. Method

Forging is done between 850–1150 °C.

The stages required for the forging process were:

- ingot forging $D = 1160$ mm in a square $750 \times 750 \times 1$ (minimum degree of deformation 1.9:1).
- cutting the foot of the ingot and the semi-finished product.
- removing the semi-finished product (starting from dimensions $750 \times 750 \times 2119$);
- adjusting the semi-finished product to the forging size.
- notching and stretching the semi-finished product for a sizing step.
- Type of heat treatment:
- Tempering: 820–860 °C/oil
- Recovery: 540–580 °C/air

Description of the heat treatment technologies applied to the studied semi-finished products.

The thermal treatments of normalization, hardening, and recovery have been carried out to obtain the quality of the analyzed semi-finished products.

A martensitic structure is obtained by hardening. Cooling is carried out at a comparatively higher speed than the steel quid speed.

The heat treatment of tempering applied to products which are called and consist of heating and maintenance at temperatures set below the transformation line so that structural conditions and voltages close to the equilibrium state are achieved, with the aim of eliminating or reducing stresses and fragility, improving tension, and reducing the hardness.

Figure 1 shows the heating range and the cycle of operations for tempering the semi-finished products, and Figure 2 shows the diagram of the heat treatment furnace used.

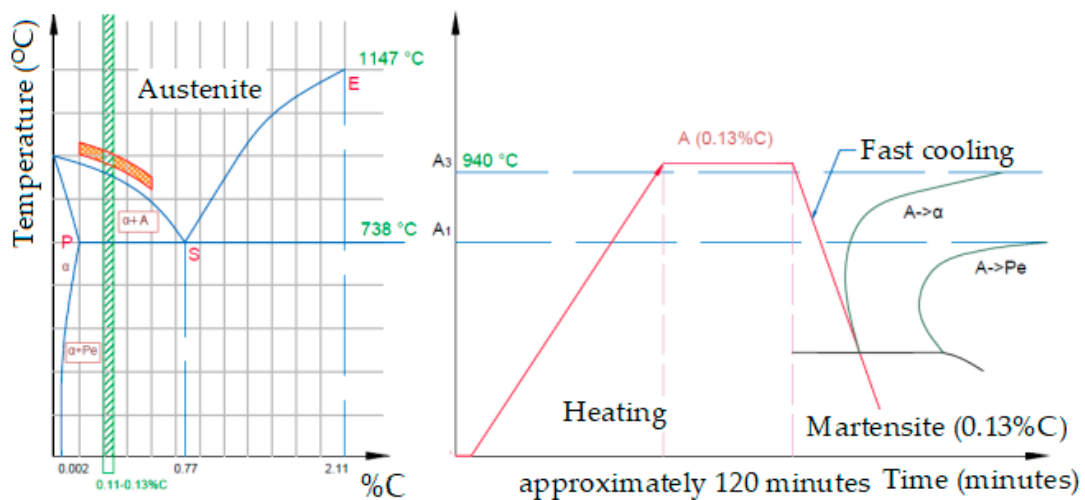


Figure 1. The heating range and the cycle of operations for tempering the semi-finished products [1].

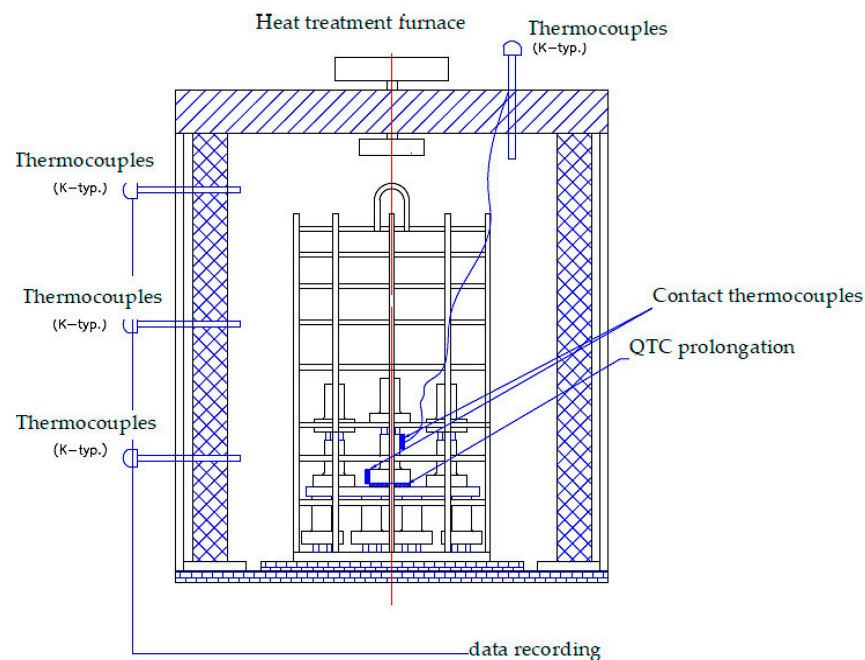


Figure 2. The heat treatment furnace [1].

2.2.1. Description of Mechanical Shock Tests—Resilience

The determination shall be made by applying a shock load from a height h on a test tube with a notch in U or V, denoted KCU or KCV. The test tubes shall be placed on the reassembly using the centering pliers so that the hammer strikes the face opposite the notch.

2.2.2. Description of the Determination of the Size of the Austenitic Grain for Forged Semi-Manufactures

The method used to highlight the austenitic grain is the method of controlled oxidation and is done as follows:

- A flat face of the sample must be sanded, and the rest must show no signs of oxidation [9,13];
- The sample is placed in the oven with the surface sanded up and is kept for 1 h at the austenite temperature provided for each quality of material; then open the oven door and leave the sample in its door for about 10–15 s for oxidation, then place the iron in water;

- In the case of significant oxidation, the oxide adhering to the polished surface is easily removed by grinding with fine sandpaper, after which the sample is attacked with Vilella reagent (1 g picric acid, 5 mL hydrochloric acid, 100 mL ethyl alcohol) [14–19]

The size index of the austenitic grain is determined on the microscope using a 100× magnification. The determination of the size index of the austenitic grain will be done by the method of comparing it with standard images.

Optical microscopy studies provide a sequence of data that attests to the influence of the chemical composition of steels on the structure but also of the changes generated by heat treatments.

In the [33] work in the list of bibliographic references, the authors demonstrated that dynamic recrystallization occurs under different hot deformation conditions, and the size of the recrystallized grains decreases with the increase of the Zener-Hollomon (Z) parameter.

The parameter Z is the deformation rate coefficient coupled with the temperature effect, with the expression $Z = \dot{\epsilon} \exp(Q/RT)$ [17], where Q is the deformation activation energy ($381.34 \text{ kJ}\cdot\text{mol}^{-1}$) [11], R is the gas constant ($8.314 \text{ J}\cdot(\text{mol}\cdot\text{K})^{-1}$) and T is the thermodynamic temperature [33].

2.2.3. Description of Metallographic Analysis—Structural Determinations

The determination of the microstructure is usually made at a magnification of ×100 or ×200 to highlight any segregations and increases of ×400 or ×500 to record the structural constituents obtained after the operation of tempering and return. The sample is taken, after which it is sanded and attacked with Nital 2%. The macrostructure is determined on samples of about 15 to 20 mm cut either from a laminate, forged, or from a piece [20–25].

The sample is rectified, degreased, and then attacked with a reagent. A mixture of 85% hydrochloric acid + 10% distilled water is usually used. The duration of the attack is one hour. After 40 min from the start of the attack, 5% oxygenated water can be put in. The area shall be examined at the magnification of ×10 (visual examination).

Following experimental research on the 3 types of analyzed steels (10CrMo9-10, 25CrMo4, and 42CrMo4), we can compare the choice of the best material as a ratio of mechanical characteristics (tests according to DNVGL-RP0034-SFC2 and NACE MR0175–Dough 207-235 HBW) and the production cycle for the three samples selected from each material as follows:

- There are different materials with different chemical compositions: 10CrMo9-10 has a lower percentage of C (0.15%) and Mn (0.55%) and more significant by Cr (2.48%), Mo (1.02%) the initial amount of Fe = 95.28%; 25CrMo4 has a higher percentage of C (0.32%) and Mn (0.73%) and lower by Cr (1.07%) and Mo (0.26%) the final amount of Fe = 96.81%; 42CrMo4 has a higher percentage of C (0.42%) and Mn (0.83%) and lower by Cr (1.04%) and Mo (0.25%) the final amount of Fe = 96.84%;
- They are regulated by different standards; therefore, 10CRMO9-10 is found in EN 10222-2 as being part of the category of ferrite and martensitic steels having specific mechanical characteristics at high temperatures, and 25CrMo4 and 42CrMo4 are both regulated by EN 10250-3 as being part of the allied special steel category.

The primary heat treatment used consists of normalization at 941–968 °C, monitoring with contact thermocouples, holding for at least 1 h after reaching the equalization temperature, and cooling to the room temperature in air.

As a secondary heat treatment for the 10CrMo9-10 material, a quenching at 940 °C with a 120 min hold and cooling in water was applied, followed by tempering at 655 °C with a 180 min hold and air cooling.

2.3. Equipment Used for Experimental Research

The equipment used in the experimental research were a Charpy shock testing machine with a low-temperature chamber, a tensile testing machine, an electronic axial strain gauge for a tensile testing machine, Spectrometer, a metallographic optical microscope, and a Brinell hardness tester.

3. Results and Discussion

3.1. Results

3.1.1. Results Obtained for the Forged Semi-Finished 10CrMo9-10

The results obtained after the mechanical tests are presented in Table 4.

Table 4. The results of the mechanical tests for 10CrMo9-10 [1].

Product		Material		HN	HN	Specification						
Forged		10CrMo9-10		91,884	11,466	ISO 6892						
Sample size (mm)		102 × 102 × 204 mm										
Mechanical characteristics												
Traction test			The impact test			Hardness						
Method												
ISO 6892-1	ISO-6892-2	-	-	ISO 148-1			ISO 6506-1					
Sampling mode	Specimen orientation	Sample size (mm)		Sample size			Temperature (°C)					
		Ø 12.5	Ø 10	10 × 10 × 55			Lateral expansion					
		x						22				
		Temperature (°C): 22			Temperature (°C): −60							
		Rp0.2 [N/mm ²]	Rm [N/mm ²]	A (%)	Z (%)	KV (J)	KV (J)	KV (J)	mm	mm	mm	HBW
1/4T	L	596	719	235	77	240	240	240	-	-	-	223

Results obtained after determining the austenitic grain index are presented in Table 5.

Table 5. The results were obtained after determining the austenitic grain index for the 10CrMo9-10 sample [1].

Current Number	Intercepts Number	Grain Size (mm)
1.	115	6
2.	141	7
3.	139	7
4.	120	6

These results were obtained under the experimental conditions presented in Table 6.

Table 6. The experimental conditions for determining the austenitic grain index for 10CrMo9-10 [1].

Material	10CrMo9-10
Method	E112-2013
Equipment	MICROSCOPE JP-6A
Objective	×100
HT	11,466
HN	91,884

Microscopic appearance of austenitic grains for the forged semi-finished product 10CrMo9-10 is presented in Figure 3.

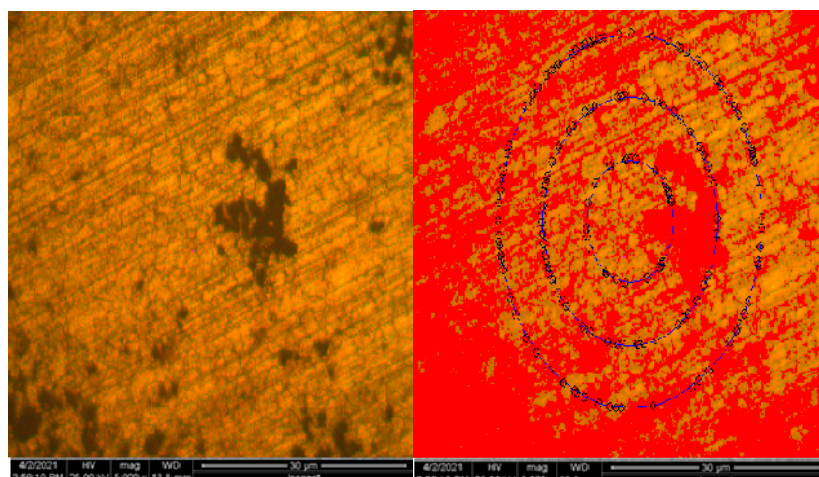


Figure 3. Microscopic appearance of austenitic grains for the forged semi-finished product 10CrMo9-10 [1].

Results obtained for structural investigations by optical microscopy are presented in Figure 4.

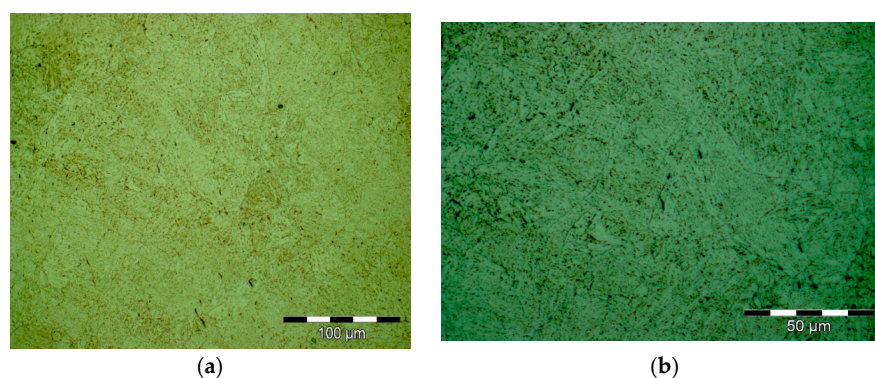


Figure 4. Optical microscopy images from secondary heat treatment; 500× magnification (a) 1000× (b).

Results obtained from the structural investigation performed by electron scanning microscopy (SEM) are presented in Figure 5.

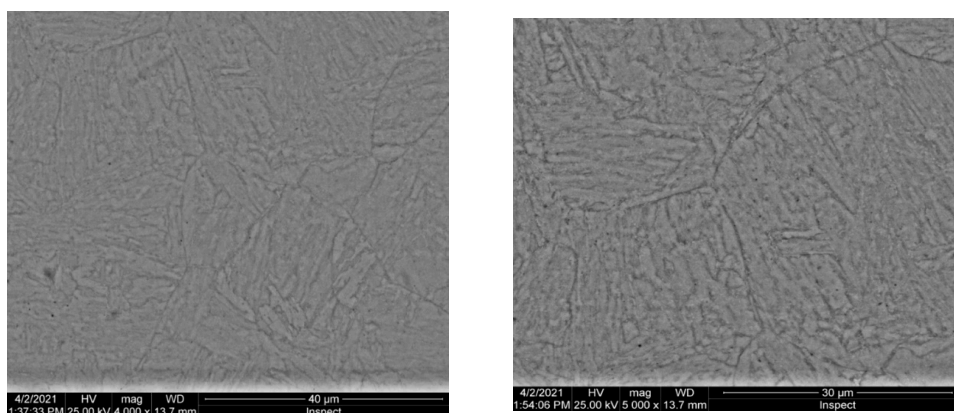


Figure 5. Electronic scanning microscopy for 10CrMo9-10 sample.

Optical microscopy studies provide a sequence of data that attests to the influence of the chemical composition of steel on the structure, as well as the changes generated by thermal treatments.

Results obtained for structural investigation of energy dispersion spectrometry (EDS), are presented in Figure 6.

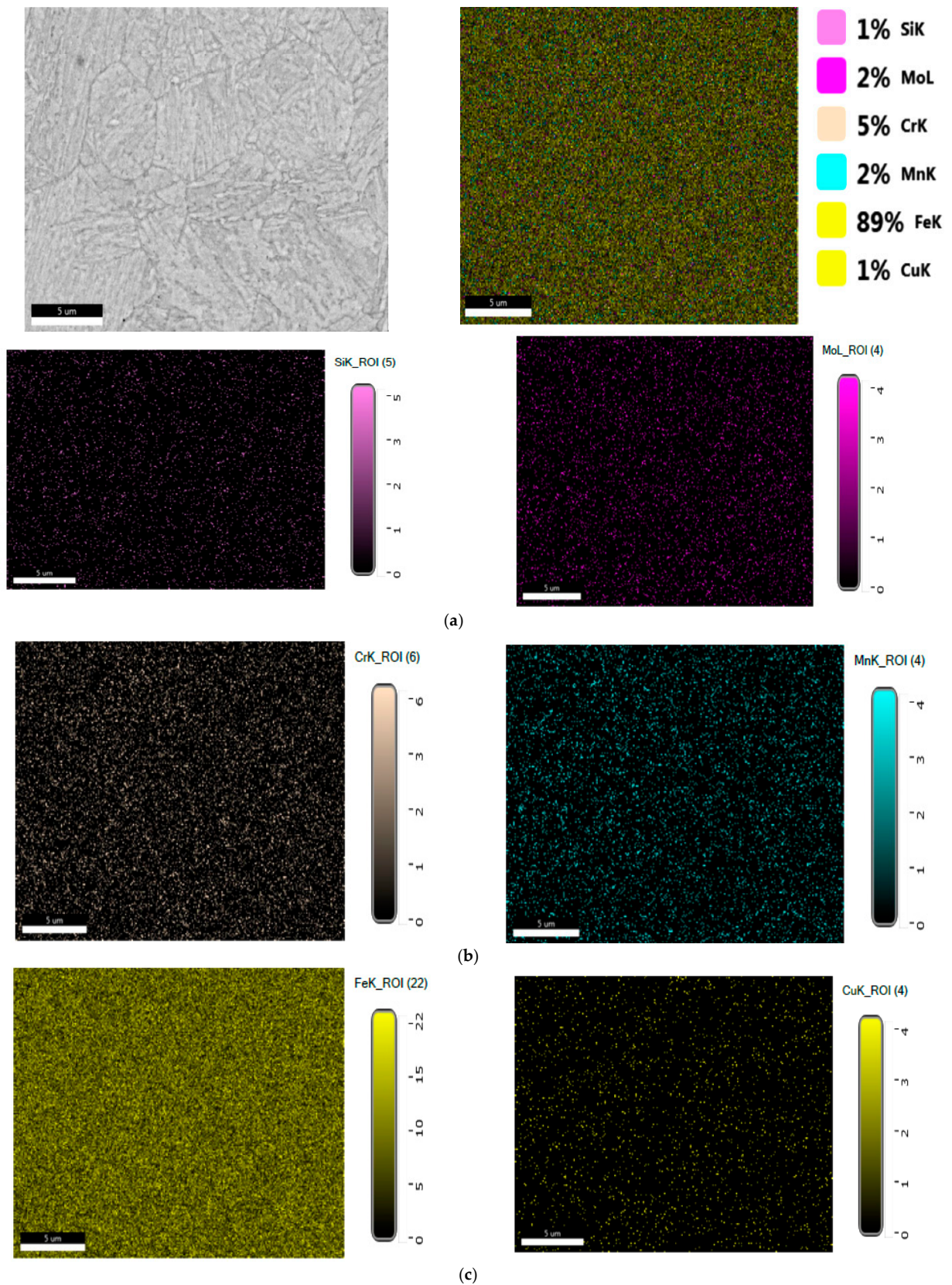
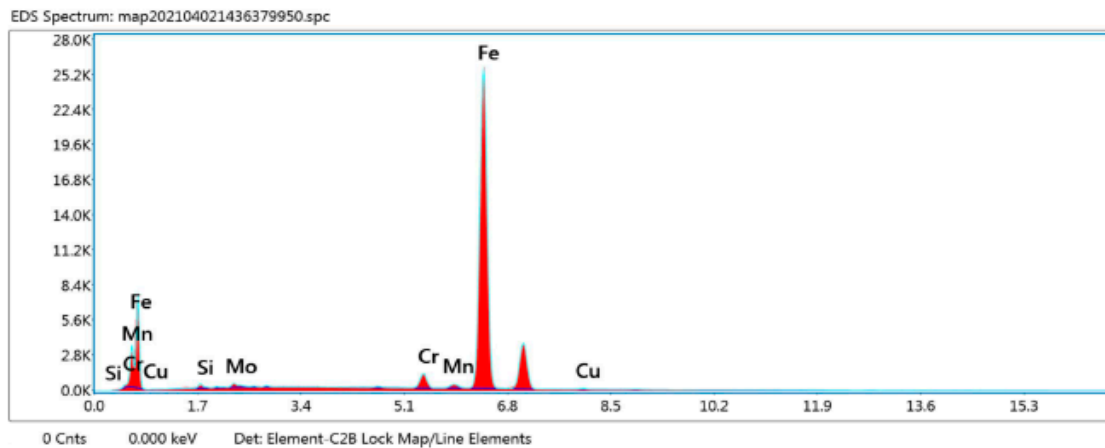


Figure 6. Cont.



Smart Quant Results

Element	Weight %	Atomic %	Net Int.	Error %	Kratio	Z	A	F
SiK	0.59	1.16	20.47	11.45	0.0025	1.1574	0.3748	1.0031
MoL	0.98	0.57	22.63	12.46	0.0071	0.9042	0.7924	1.0018
CrK	2.85	3.05	111.72	3.81	0.0320	1.0014	0.9829	1.1389
MnK	0.53	0.54	18.44	13.59	0.0058	0.9824	0.9913	1.1155
FeK	94.62	94.31	2717.75	1.25	0.9387	1.0003	0.9909	1.0008
CuK	0.42	0.37	7.64	24.58	0.0036	0.9670	0.8692	1.0099

(d)

Figure 6. (a) EDS spectrum for the Si element from the 10CrMo9-10 steel sample. (b) EDS spectrum for the Cr element from the 10CrMo9-10 steel sample. (c) EDS spectrum for the Fe element from the 10CrMo9-10 steel sample. (d) The spot chemical analysis in the selected area for the 10CrMo9-10 steel sample.

3.1.2. Results Obtained for the Forged Semi-Finished 25CrMo4

The results obtained after the mechanical tests are presented in Table 7.

Table 7. The results of the mechanical tests for 25CrMo4 [1].

Product		Material		HN	HN	Specification						
Forged		25CrMo4		51,185	50,531	ISO 6892						
Sample size (mm)		102 × 102 × 204										
Mechanical characteristics												
Traction test			The impact test			Hardness						
Method												
ISO 6892-1	ISO-6892-2	-	-	ISO 148-1		ISO 6506-1						
Sampling mode	Specimen orientation	Sample size (mm)		Sample size		Temperature (°C)						
		Ø 12.5	Ø 10	10 × 10 × 55	Lateral expansion	22						
		Temperature (°C): 22					Temperature (°C): -60					
		Rp0.2 [N/mm ²]	Rm [N/mm ²]	A (%)	Z (%)	KV (J)	KV (J)	KV (J)	mm	mm	mm	HBW
1/4T	L	597	728	255	705	240	240	240	-	-	-	235

Results obtained after determining the austenitic grain index are presented in Table 8.

Table 8. The results were obtained after determining the austenitic grain index for the 25CrMo4 sample [1].

Current Number	Intercepts Number	Grain Size (mm)
1.	139	7
2.	139	7
3.	128	7
4.	123	6

These results were obtained under the experimental conditions presented in Table 9.

Table 9. The experimental conditions for determining the austenitic grain index for 25CrMo4 [1].

Material	25CrMo4
Method	E112-2013
Equipment	MICROSCOPE JP-6A
Objective	×100
HT	50,531
HN	51,185

Microscopic appearance of austenitic grains for the forged semi-finished product 10CrMo9-10 is presented in Figure 7.

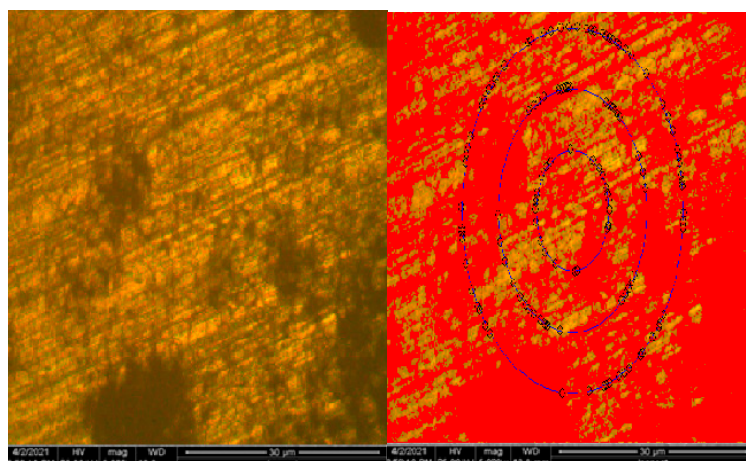


Figure 7. Microscopic appearance of austenitic grains for the forged semi-finished product 25CrMo4 [1].

Results obtained for structural investigations by optical microscopy are presented in Figure 8.

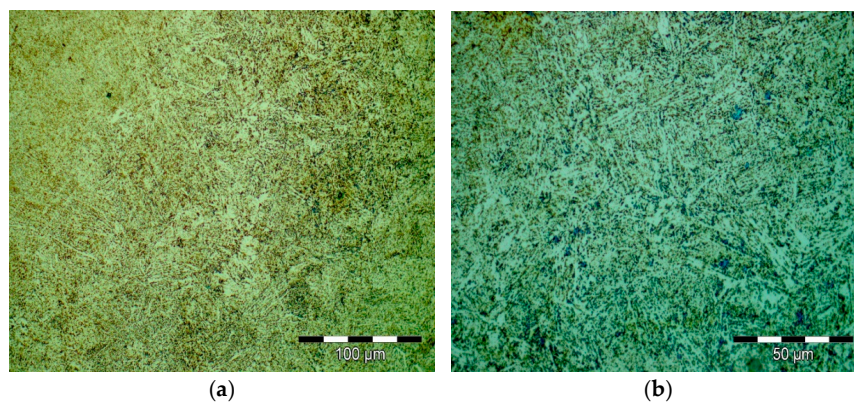


Figure 8. Optical microscopy images from secondary heat treatment; 500× magnification (a) 1000× (b).

Results obtained from the structural investigation performed by electronic scavenging microscopy (SEM) are presented in Figure 9.

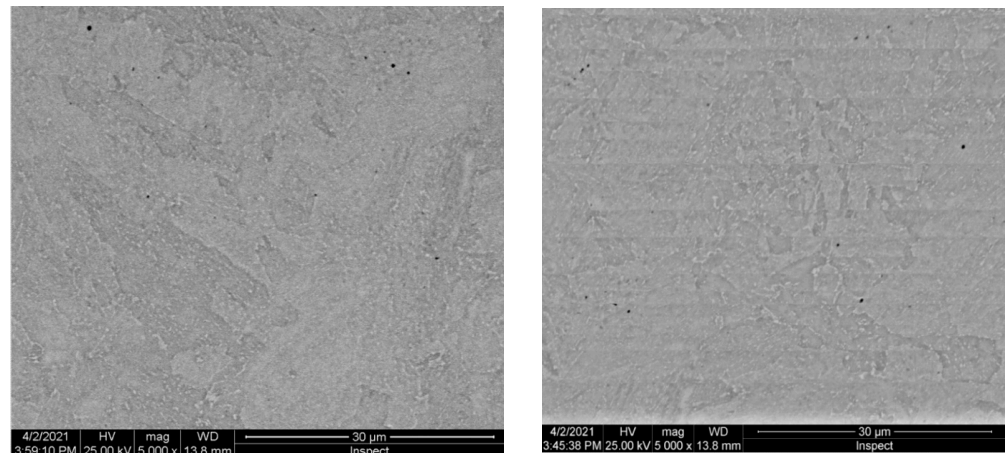


Figure 9. Electronic scanning microscopy for 25CrMo4 steel sample.

Optical microscopy studies provide a sequence of data that attests to the influence of the chemical composition of steel on the structure, as well as the changes generated by thermal treatments.

Results obtained from structural investigation of energy dispersion spectrometry (EDS), are presented in Figure 10.

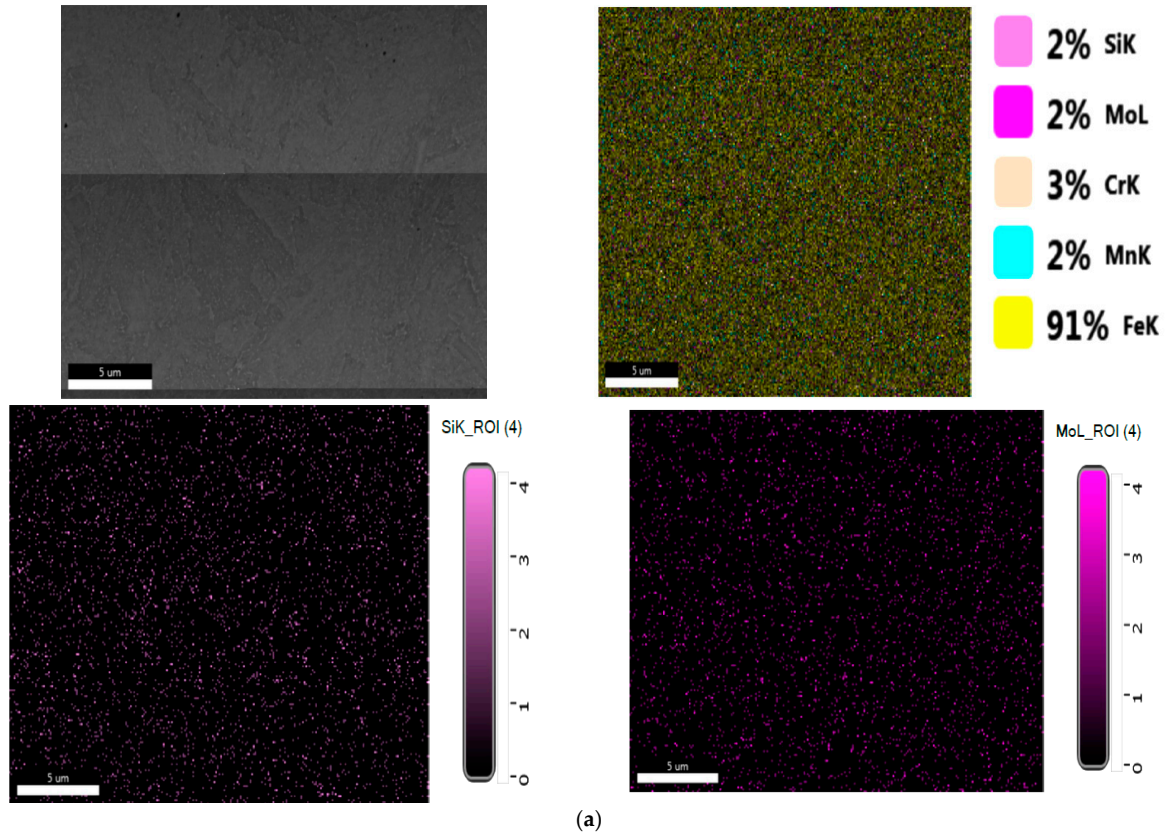
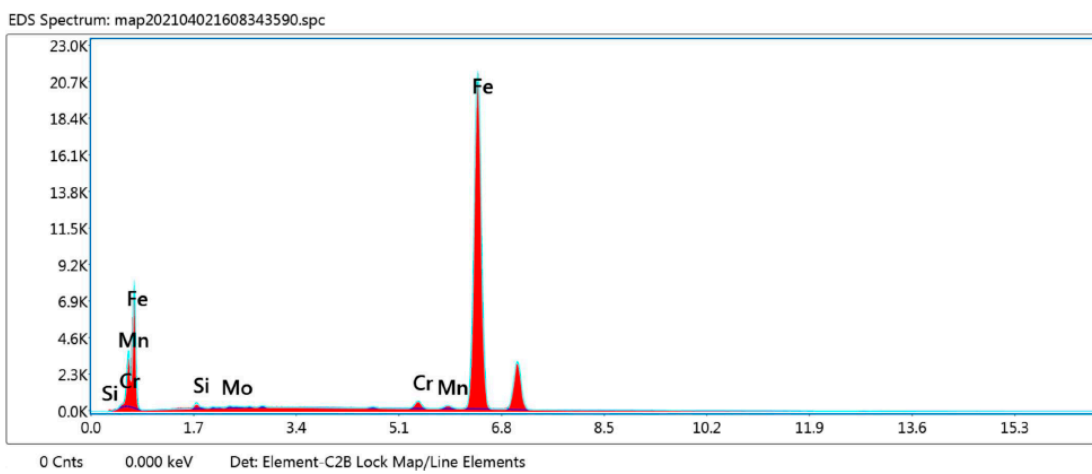
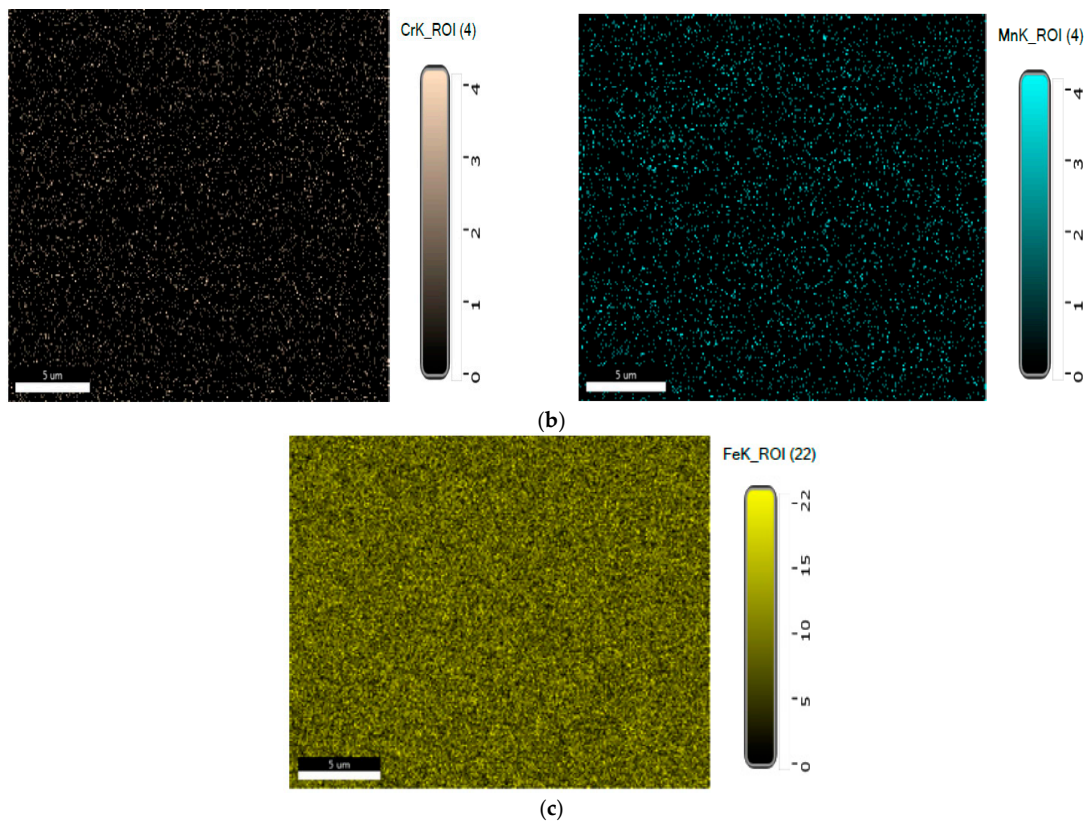


Figure 10. Cont.



Smart Quant Results

Element	Weight %	Atomic %	Net Int.	Error %	Kratio	Z	A	F
SiK	0.83	1.63	23.27	11.20	0.0036	1.1561	0.3743	1.0030
MoL	0.42	0.24	7.70	20.48	0.0030	0.9032	0.7900	1.0018
CrK	1.43	1.53	45.75	7.54	0.0162	1.0003	0.9838	1.1487
MnK	0.53	0.53	14.98	18.44	0.0058	0.9813	0.9926	1.1262
FeK	96.80	96.07	2252.10	1.23	0.9628	0.9991	0.9953	1.0002

(d)

Figure 10. (a) EDS spectrum for the Si element from the 25CrMo4 steel sample. (b) EDS spectrum for the Cr element from the 25CrMo4 steel sample. (c) EDS spectrum for the Fe element from the 25CrMo4 steel sample. (d) The spot chemical analysis in the selected area for the 25CrMo4 sample.

3.1.3. Results Obtained for the Forged Semi-Finished 42CrMo4

The results obtained after the mechanical tests are presented in Table 10.

Table 10. The results of the mechanical tests for 42CrMo4 [1].

Product		Material		HN	HN	Specification						
Forged		42CrMo4		92,083	11,606	ISO 6892						
Sample size (mm)		102 × 102 × 204										
Mechanical characteristics												
Traction test			The impact test			Hardness						
Method												
ISO 6892-1	ISO-6892-2	-	-	ISO 148-1		ISO 6506-1						
Sampling mode	Specimen orientation	Sample size (mm)		Sample size			Temperature (°C)					
		Ø 12.5	Ø 10	10 × 10 × 55		Lateral expansion	22					
		x										
		Temperature (°C): 22			Temperature (°C): −60							
		Rp0.2 [N/mm ²]	Rm [N/mm ²]	A (%)	Z (%)	KV (J)	KV (J)	KV (J)	mm	mm	mm	HBW
1/4T	L	607	784	215	62	212	220	215	-	-	-	229

Results obtained after determining the austenitic grain index are presented in Table 11.

Table 11. The results were obtained after determining the austenitic grain index for the 42CrMo4 sample [1].

Current Number	Intercepts Number	Grain Size (mm)
1.	161	7
2.	161	7
3.	173	7
4.	165	7

These results were obtained under the experimental conditions presented in Table 12.

Table 12. The experimental conditions for determining the austenitic grain index for 42CrMo4 [1].

Material	42CrMo4
Method	E112-2013
Equipment	MICROSCOPE JP-6A
Objective	×100
HT	11,606
HN	92,083

Microscopic appearance of austenitic grains for the forged semi-finished product 42CrMo4 is presented in Figure 11.

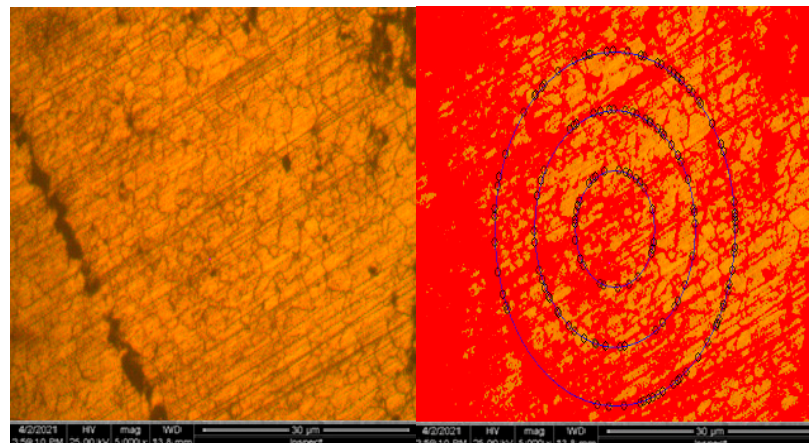


Figure 11. Microscopic appearance of austenitic grains for the forged semi-finished product 42CrMo4 [1].

Results obtained for structural investigations by optical microscopy are presented in Figure 12.

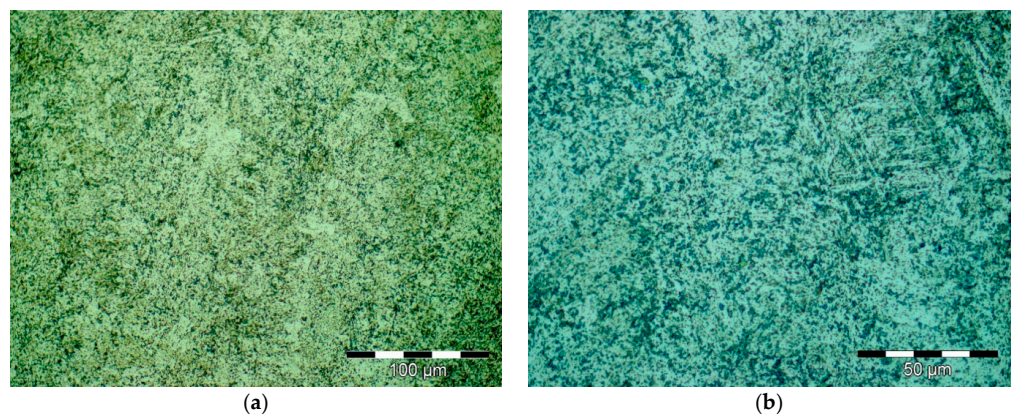


Figure 12. Optical microscopy images from secondary heat treatment; 500× magnification (a) 1000× (b).

Results obtained from the structural investigation performed by electronic scanning microscopy (SEM) are presented in Figure 13.

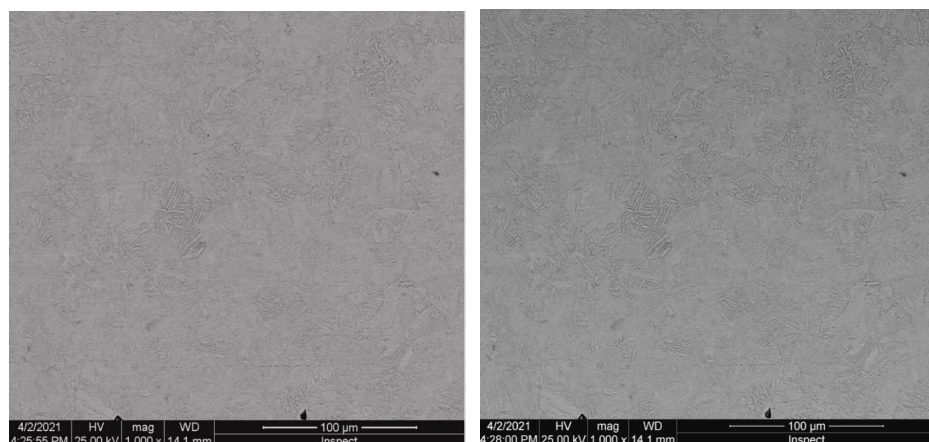


Figure 13. Electronic scanning microscopy for 42CrMo4 sample.

Optical microscopy studies provide a sequence of data that attests to the influence of the chemical composition of steel on the structure, as well as the changes generated by thermal treatments.

Results obtained for structural investigation of energy dispersion spectrometry (EDS), are presented in Figure 14.

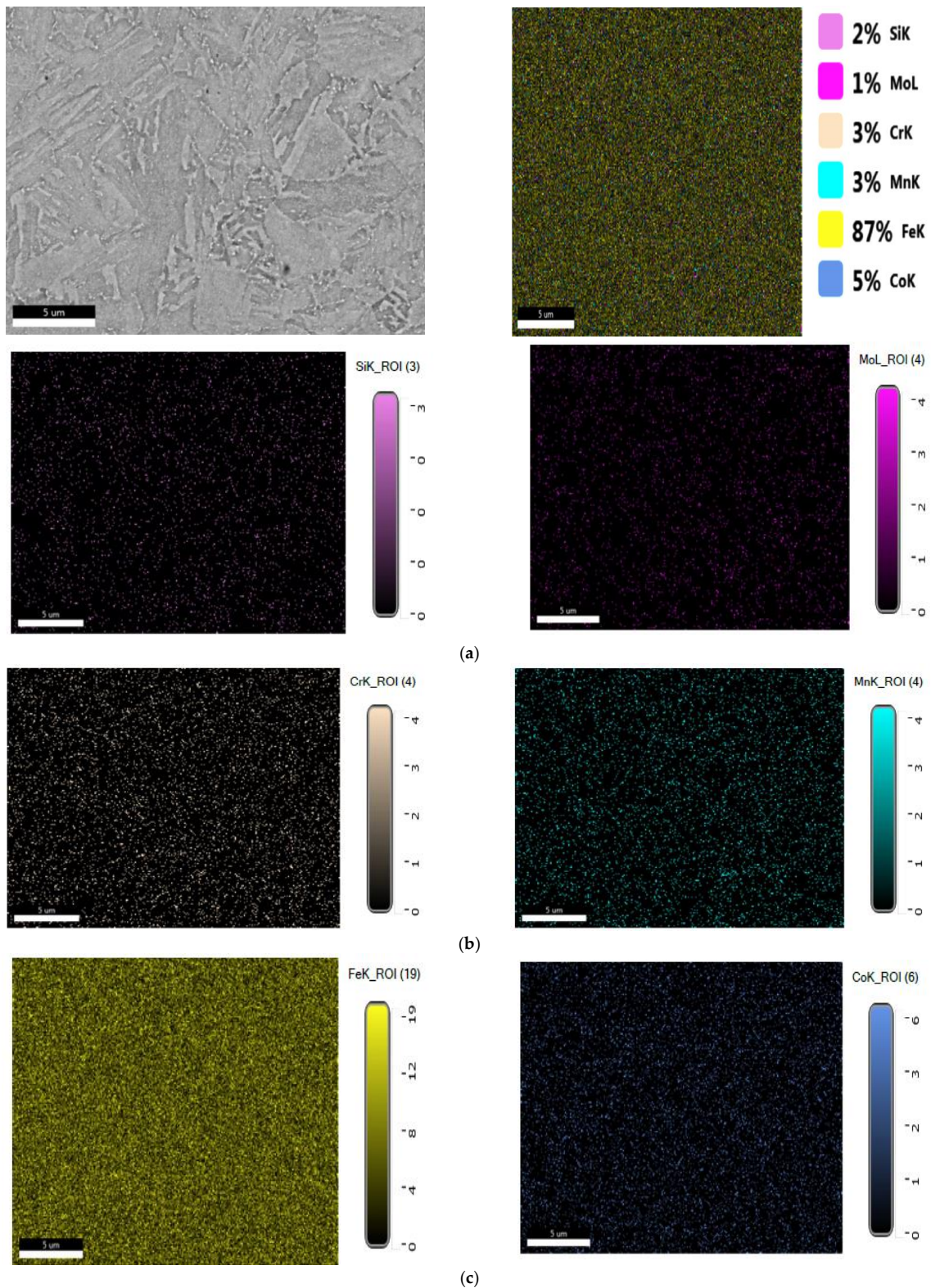


Figure 14. Cont.

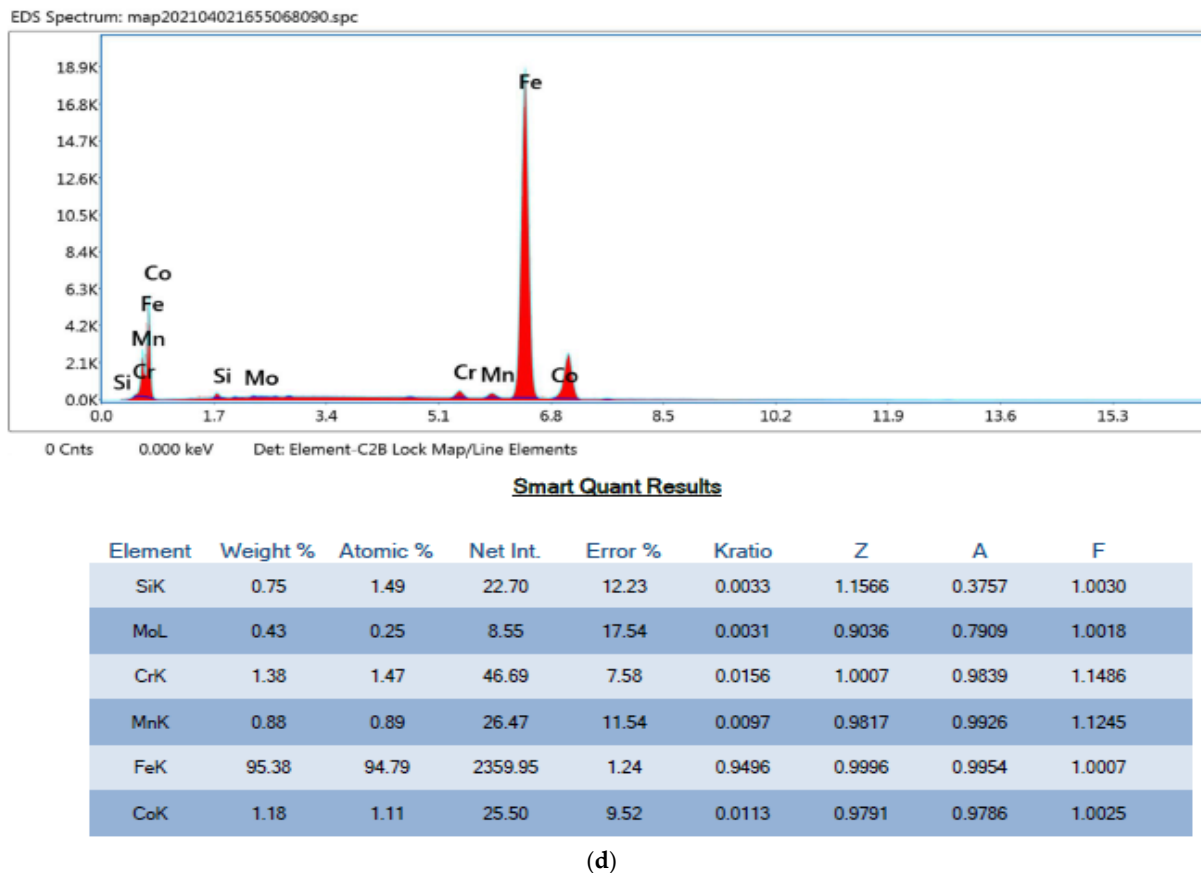


Figure 14. (a) EDS spectrum for the Si element from the 42CrMo4 steel sample. (b) EDS spectrum for the Cr element from the 42CrMo4 steel sample. (c) EDS spectrum for the Fe element from the 42CrMo4 steel sample. (d) The spot chemical analysis in the selected area for 42CrMo4 sample.

3.2. Discussion

To choose the best forging and heat treatment parameters, a comparative study was carried out for 3 analyzed steel samples, 10CrMo9-10, 25CrMo4, and 42CrMo4.

They are the usual heat-resistant alloy steel used in various national and international industries with specific applications at high temperatures and breaking energy down to a temperature of $-80\text{ }^{\circ}\text{C}$.

This comparative study aims to establish the best forging parameters and thermal treatment to obtain the best ratio between the mechanical characteristics obtained and the parameters of the forged semi-finance cycle.

The primary heat treatment used in the presented technology for the 10CRMo9-10 material was normalization at $941\text{--}968\text{ }^{\circ}\text{C}$, monitoring with contact thermocouples, holding for at least 1 h after reaching the equalization temperature, and cooling to room temperature in air.

As a secondary heat treatment for this manufacturing technology, a quenching at $940\text{ }^{\circ}\text{C}$ with a 120 min hold and cooling in water was applied to the 10CRMo9-10 material, followed by a return to $655\text{ }^{\circ}\text{C}$, a 180 min hold and air cooling.

As the parameters of the forging process and thermal treatments are relatively similar, as a maintenance interval, the highest values we find are 25CrMo4 (300 min for quenching and 600 min at high return), 42CrMo4 (120 min for hardening and 120 min at Return), and 10CrMo9-10 (60 min for both hardening and reversing).

For the material 42CrMo4 (steel alloyed with Cr and Mo), the same parameters were used for 10CrMo9-10: forging temperature $1150\text{ }^{\circ}\text{C}$ (forging end temperature above $850\text{ }^{\circ}\text{C}$), ingot 25 tons with the application of primary heat treatment of normalization.

These results were obtained under the experimental conditions presented in Table 13.

Table 13. The results were obtained under experimental conditions.

Steel Brands	R _m , N/mm ²	R _{p0.2} , N/mm ²	A, %	Z, %	KV	HBV
10CRMo9-10	697	577	24	76	240	217
42CrMo4	843	512	15	31	210	255

After applying the secondary heat treatment, an improved structure favorable for mechanical processing appears; it is no longer prone to cracks or the appearance of intergranular inclusions, harder but a little more fragile than the one obtained from 10CrMo9-10 (following the application of the same MPS technology).

The same technology was applied to a 25CrMo4 semi-finished product: 1150 °C as forging temperature and finally, secondary heat treatment at 860 °C with maintenance after 60 min equalization and cooling in water followed by a return to 550 °C with 120 min maintenance and cooling in the air.

The mechanical characteristics obtained are relatively close to the highest.

The elongation and the cooking have little lower values as the next 10CrMo4; thus, $a = 24\%$ and $z = 66\%$. The breaking energy is identical to all three analyzed samples. As a characteristic of steels involving an analysis of R_m and R_{p0.2}, it represents ductility (ratio between $r_m/r_{p0.2}$). In the case of steel 10CrMo9-10 ductility = $r_m/r_{p0.2} = 1.21$; for 25CrMo4 ductility = 1.25; for 42CrMo4 ductility = 1.27.

Considering all these aspects, it can be accepted that the 42CrMo4 sample has superior characteristics to the other steel brands tested.

The 10CrMo9-10 steel grade can be considered for use at high temperatures, which has lower forging and heat treatment costs than the other tested steel brands.

The results of the conducted research recommend the large-scale use of semi-finished products made of steel brand 10CrMo9-10.

The following conclusions can be drawn from the tests carried out on 42CrMo4 and 25CrMo4 steels:

The DNV-GL-ST-F101 is widely used in the field of metallurgy, especially forged semi-finished products in the field of extraction, natural gas, petroleum, and maritime. The procedure for issuing a certificate of material with international recognition of DNV-G type 3.2 involves meeting essential criteria both in the fields of forging and thermal treatment.

4. Conclusions

As a result of the forging process, it was observed that the strength and the deformation velocity (vectorial quantity) decrease with the increase in temperature.

After applying the secondary heat treatment, an improved structure favorable for mechanical processing appears; it is no longer prone to cracks or the appearance of intergranular inclusions.

The variation of austenitic grain size depends on the concentration of alloying elements and temperature; for the benchmark forged at 1150 °C from 42CrMo4, a coarse structure consisting of lamellar pearlite, bainite, and ferrite in reduced proportions was found.

The final value of the mechanical characteristics depends on the type of operations in the technological flow: free forging, the type of primary heat treatment, the type of secondary heat treatment, and the chemical composition and alloying elements of the steels used.

Experimental laboratory research shows that the 42CrMo4 steel has the highest value of mechanical characteristics, and the 10CrMo9-10 steel presents the best value for plasticity.

The 42CrMo4 brand steel sample presented the best metallographic structure, forged at 1150 °C, where a rough structure consisting of lamella, bainite, and ferrite in small proportions was found.

- Both the forging technique and the types of heat treatment applied are important to meet the requirements of the evaluation norm and offer the possibility of issuing an internationally recognized quality certificate.
- The obtained results can be used to establish different technologies for the elaboration of steels from the analyzed materials at the national and international industrial levels.

Author Contributions: Conceptualization, N.C., V.C.; Methodology, V.C.; Software, V.R.; Formal analysis, A.I. (Adrian Ioana); Investigation, V.C.; Resources, C.D.; Data curation, A.I. (Alexandra Istrate); Formal analysis, V.P. All authors have read and agreed to the published version of the manuscript.

Funding: This work was supported by Programul Operational Capital Uman, Axa prioritară 6—Educațieș competente, Proiect: Pregătirea doctoranzilor și cercetătorilor postdoctorat în vederea dobândirii de competente de cercetare aplicativă—SMART Cod MySMIS: 153734, and the authors would want to thank University “Politehnica” of Bucharest for the chance to publish this paper.

Institutional Review Board Statement: Not applicable.

Informed Consent Statement: Not applicable.

Data Availability Statement: Not applicable.

Conflicts of Interest: The authors declare no conflict of interest. The funders had no role in the study’s design; in the collection, analyses, or interpretation of data; in the writing of the manuscript, or in the decision to publish the results.

References

1. Caloian, V. Experimental Research for Establishment of the Optimum Technology for the Execution of Forged Semi-Products with Special Destination, Politehnica. Ph.D. Thesis, University of Bucharest, Bucharest, Romania, 2021.
2. Du, F.; Zhou, P.; Guo, P.; Li, C.; Deng, L.; Wang, X.; Jin, J. Effect of Hot Deformation Parameters on Heat-Treated Microstructures and Mechanical Properties of 300M Steel. *Materials* **2022**, *15*, 8927. [[CrossRef](#)] [[PubMed](#)]
3. Qian, D.S.; Peng, Y.Y. Effects of forming parameters on coupled thermomechanical behaviours in combined ring rolling. *Ironmak. Steelmak. Process. Prod. Appl.* **2015**, *42*, 471–480. [[CrossRef](#)]
4. Liu, X.-J.; Liao, S.-M.; Rao, Z.-H.; Liu, G. An input–output model for energy accounting and analysis of industrial production processes: A case study of an integrated steel plant. *J. Iron Steel Res. Int.* **2018**, *25*, 524–538. [[CrossRef](#)]
5. Lu, J.-L.; Cheng, G.-G.; Wu, M.; Yang, G.; Che, J.-L. Detection and analysis of magnetic particle testing defects on heavy truck crankshaft manufactured by microalloyed medium-carbon forging steel. *J. Iron Steel Res. Int.* **2020**, *27*, 608–616. [[CrossRef](#)]
6. Zhu, S.; Peng, W.-F.; Shu, X.-D. Effect of tempering on bonding characteristics of cross wedge rolling 42CrMo/Q235 laminated shafts. *J. Iron Steel Res. Int.* **2020**, *27*, 1170–1178. [[CrossRef](#)]
7. Sun, C.; Yang, S.-W.; Zhang, R.; Wang, X.; Guo, H. Influence of plastic deformation on thermal stability of low carbon bainitic steel. *J. Iron Steel Res. Int.* **2015**, *22*, 60–66. [[CrossRef](#)]
8. Kim, S.H.; Yeon, S.-M.; Lee, J.H.; Kim, Y.W.; Lee, H.; Park, J.; Lee, N.-K.; Choi, J.P.; Jr, C.A.; Lee, Y.J.; et al. Additive manufacturing of a shift block via laser powder bed fusion: The simultaneous utilisation of optimised topology and a lattice structure. *Virtual Phys. Prototyp.* **2020**, *15*, 460–480. [[CrossRef](#)]
9. Di Schino, A.; Gaggiotti, M.; Testani, C. Heat Treatment Effect on Microstructure Evolution in a 7% Cr Steel for Forging. *Metals* **2020**, *10*, 808. [[CrossRef](#)]
10. Mengaroni, S.; Cianetti, F.; Calderini, M.; Evangelista, E.; Di Schino, A.; McQueen, H. Tool Steels: Forging Simulation and Microstructure Evolution of Large-Scale Ingot. *Acta Phys. Pol. A* **2015**, *128*, 629–633. [[CrossRef](#)]
11. Morales-Cruz, E.; Vargas-Ramírez, M.; Lobo-Guerrero, A.; Cruz-Ramírez, A.; Colin-García, E.; Sánchez-Alvarado, R.; Gutiérrez-Pérez, V.; Martínez-Vázquez, J. Effect of low aluminum additions in the microstructure and mechanical properties of hot forged high-manganese steels. *J. Min. Met. Sect. B Met.* **2023**, *7*. [[CrossRef](#)]
12. Santosh, S.; Sampath, V.; Mouliswar, R. Hot deformation characteristics of NiTiV shape memory alloy and modeling using constitutive equations and artificial neural networks. *J. Alloys Compd.* **2022**, *901*, 163451. [[CrossRef](#)]
13. Lv, Y.; Zhao, S.; Liu, T.; Cheng, H.; Fan, J.; Huang, Y. Hot Deformation Behavior and Simulation of Hot-Rolled Damage Process for Fine-Grained Pure Tungsten at Elevated Temperatures. *Materials* **2022**, *15*, 8246. [[CrossRef](#)]
14. Yang, C.; Hu, Z. Research on the ovality of hollow shafts in cross wedge rolling with mandrel. *Int. J. Adv. Manuf. Technol.* **2016**, *83*, 67–76. [[CrossRef](#)]
15. Santosh, S.; Praveen, R.; Sampath, V. Influence of Cobalt on the Hot Deformation Characteristics of an NiTi Shape Memory Alloy. *Trans. Indian Inst. Met.* **2019**, *72*, 1465–1468. [[CrossRef](#)]

16. Artyukhova, N.; Anikeev, S.; Promakhov, V.; Korobekov, M. The Effect of Cobalt on the De-formation Behaviour of a Porous TiNi-Based Alloy Obtained by Sintering. *Materials* **2021**, *14*, 7584. [[CrossRef](#)]
17. Liu, T.; Long, M.-J.; Chen, D.-F.; Duan, H.-M.; Gui, L.-T.; Yu, S.; Cao, J.-S.; Chen, H.-B.; Fan, H.-L. Effect of coarse TiN inclusions and microstructure on impact toughness fluctuation in Ti micro-alloyed steel. *J. Iron Steel Res. Int.* **2018**, *25*, 1043–1053. [[CrossRef](#)]
18. Li, X.; Bao, Y.; Wang, M. Peeling defects of cold rolled interstitial-free steel sheet due to inclusion movement. *Ironmak. Steelmak. Process. Prod. Appl.* **2020**, *47*, 1–5. [[CrossRef](#)]
19. Yang, C.; Ma, J.; Hu, Z. Analysis and design of cross wedge rolling hollow axle sleeve with mandrel. *J. Mater. Process. Technol.* **2017**, *239*, 346–358. [[CrossRef](#)]
20. Liu, G.Y.; Dong, L.M.; Wang, K.K.; Zhu, D.M.; Zhang, S.J.; Gong, S.C.; Li, M.W. Water–air online quenching process of 3Cr2Mo steel based on numerical simulation. *Ironmak. Steelmak.* **2016**, *43*, 780–789. [[CrossRef](#)]
21. Zhou, J.; Jia, Z.; Liu, H.; Wang, M. A study on simulation of deformation during roll-forging process using system of special shaped and hat groove. *Rev. Adv. Mater. Sci.* **2013**, *33*, 354–359.
22. Zhuang, W.; Hua, L.; Wang, X.; Liu, Y.; Han, X.; Dong, L. Numerical and experimental investigation of roll-forging of automotive front axle beam. *Int. J. Adv. Manuf. Technol.* **2015**, *79*, 1761–1777. [[CrossRef](#)]
23. Zhuang, W.; Hua, L.; Wang, X.; Liu, Y.; Dong, L.; Dai, H. The influences of process parameters on the preliminary roll-forging process of the AISI-1045 automobile front axle beam. *J. Mech. Sci. Technol.* **2016**, *30*, 837–846. [[CrossRef](#)]
24. Bulzak, T.; Tomczak, J.; Pater, Z. Theoretical and Experimental Research on Forge Rolling Process of Preforms from Magnesium Alloy AZ31. *Arch. Met. Mater.* **2015**, *60*, 437–443. [[CrossRef](#)]
25. Caloian, V.E.; Constantin, N.; Ioana, A.; Vlad, M.E. The procedure for drawing up specifications for flanged forged semi-finished products of A694F65 with special purpose for naval systems. In Proceedings of the 14th International Research Conference, International Conference on Applied Mechanics and Materials Engineering, IRC, Lisbon, Portugal, 16–17 April 2020. Available online: <https://waset.org/applied-mechanics-and-materials-engineering-conference-in-april-2020-in-lisbon> (accessed on 14 March 2023).
26. Caloian, V. Experimental research on the procedure for the preparation of standardized forged. *U.P.B. Sci. Bull. Ser. B* **2019**, *81*, 253–262.
27. Caloian, V.; Constantin, N.; Vlad, M. The influence of heating temperature and cooling rate after free forging on the micro-structure and the mechanical properties of 42CRMO4 Steel. *U.P.B. Sci. Bull. Ser. B* **2019**, *81*, 173–182.
28. Zhang, J.-T.; Zhao, Y.-G.; Tan, J.; Xu, X.-F. Austenite Grain Refinement by Reverse $\alpha' \rightarrow \gamma$ Transformation in Metastable Austenitic Manganese Steel. *J. Iron Steel Res. Int.* **2015**, *22*, 157–162. [[CrossRef](#)]
29. Kwon, S.-H.; Hong, D.-G.; Yim, C.-H. Prediction of hot ductility of steels from elemental composition and thermal history by deep neural networks. *Ironmak. Steelmak. Process. Prod. Appl.* **2020**, *47*, 1176–1187. [[CrossRef](#)]
30. Zhao, J.; Zuo, H.; Wang, Y.; Wang, J.; Xue, Q. Review of green and low-carbon ironmaking technology. *Ironmak. Steelmak. Process. Prod. Appl.* **2020**, *47*, 296–306. [[CrossRef](#)]
31. Ren, Z.; Xiao, H.; Liu, X.; Wang, G. Experimental and theoretical analysis of roll flattening in the deformation zone for ultra-thin strip rolling. *Ironmak. Steelmak. Process. Prod. Appl.* **2018**, *45*, 805–812. [[CrossRef](#)]
32. Manwatkar, S.K.; Sunil, M.; Prabhu, A.; Murty, S.V.S.N.; Joseph, R.; Narayanan, P.R. Effect of Grain Size on the Mechanical Properties of Aluminum Alloy AA2219 Parent and Weldments at Ambient and Cryogenic Temperature. *Trans. Indian Inst. Met.* **2019**, *72*, 1515–1519. [[CrossRef](#)]
33. Tao, C.; Huang, H.; Zhou, G.; Zheng, B.; Zuo, X.; Chen, L.; Yuan, X. Anomalous Hot Deformation Behavior and Microstructure Evolution of As-Cast Martensitic Niti Alloy During Hot Compression. Available online: <https://ssrn.com/abstract=4153247> (accessed on 14 June 2016).

Disclaimer/Publisher’s Note: The statements, opinions and data contained in all publications are solely those of the individual author(s) and contributor(s) and not of MDPI and/or the editor(s). MDPI and/or the editor(s) disclaim responsibility for any injury to people or property resulting from any ideas, methods, instructions or products referred to in the content.